AN OPTIMAL CONTROL SCHEME FOR A DRIVING SIMULATOR

Hatem Elloumi, Marc Bordier, Nadia Maïzi
Centre de Mathématiques Appliquées, École des Mines de Paris
2004 route des Lucioles, 06902 Sophia Antipolis Cedex, France

Keywords: Driving simulation, optimal motion cueing, Gough-Stewart platform, motion perception.

Abstract: Within the framework of driving simulation, control is a key issue to providing the driver realistic motion cues. Visual stimulus (virtual reality scene) and inertial stimulus (platform motion) induce a self-motion illusion. The challenge is to provide the driver with the sensations he would feel in real car maneuvering. This is an original control problem. Indeed, the first goal is not classical path tracking but fooling the driver awareness. Constrained workspace is the second issue classically addressed by motion cueing algorithms. The purpose of this paper is to extend the works of Telban and Cardullo on the optimal motion cueing algorithm. A nonlinear dynamical model of the robot is brought in. The actuator forces are directly included in the optimal control scheme. Consequently a better (global) optimization and an advanced parametrization of the control are achieved.

1 INTRODUCTION

Driving simulators are dedicated to the reproduction of the behavior and environment of vehicles. They use a motion system in order to provide drivers with the appropriate inertial, proprioceptive and tactile motion cues. Figure 1 shows a car cockpit mounted on a 6 degree-of-freedom parallel robot (the Gough-Stewart platform). Figure 2 depicts the robot architecture. A virtual reality environment is used to simulate the road and traffic as well.

The Gough-Stewart platform is nowadays the most common simulation platform[1] thanks to its ability to manipulate heavy weights at high speeds, its stiffness and its sensor accuracy. However it raises three issues: the coupling between the actuators, the nonlinear dynamics and the limited strokes.

The last point is, by far, the most important in the simulation context. Indeed, examine for instance the Renault simulator values (Reymond et al, 2000): the robot "allows maximum displacements up to $\pm$*20cm* and $\pm$*15deg* in all linear and angular axes". Furthermore, the platform is also limited in acceleration and speed: it can achieve *up to* $\pm$*0.5g* (g=*9.8*s^{-2} is the gravity constant) and *0.4*ms^{-1} for linear motion and *300deg*s^{-2} and *30deg*s^{-1} for angular motion. These values point out a high level of displacement limitation. Fortunately, thanks to the immersion of the driver in a virtual environment and the use of perceptual fooling it is possible to go beyond these limits, i.e., the limited robot trajectories in the virtual simulator world can provide (up to a certain point) the same feeling as a real car ride.

Consequently, the vehicle simulation community (driving, flight or motorcycle) has developed a scheme based on motion cueing algorithms (or washout filters). The two-block diagram in the top of figure 3 illustrates this idea. It consists in transforming (filtering) the real vehicle trajectories onto robot feasible ones. This projection takes into account both the constrained workspace and the satisfaction of perceptual validity. Then the simulator trajectories computed from the washout filter are performed by the robot thanks to a classical tracking algorithm.

The optimal motion cueing algorithm has been proposed by Sivan et al 1982, later implemented by Reid and Nahon 1985, and recently modified and implemented by Telban and Cardullo (Telban et al, 1999; Cardullo et al, 1999), (Telban and Cardullo, 2002), (Guo et al, 2003) for flight simulators.

[1]Used by: *Renault simulator, NASA Langley flight simulator, National Advanced Driving Simulator at the Iowa University, Airbus A340 simulator, MORIS motorcycle simulator*, etc.

Elloumi H., Bordier M. and Mäızi N. (2005).
AN OPTIMAL CONTROL SCHEME FOR A DRIVING SIMULATOR.
In *Proceedings of the Second International Conference on Informatics in Control, Automation and Robotics - Robotics and Automation*, pages 40-47
DOI: 10.5220/0001178600400047

Figure 1: Renault dynamic simulator (Reymond et al, 2000)

The idea of this paper is to unify the washout block with its tracking control neighbor in order to achieve a better (global) optimization and to investigate the nonlinear dynamics contribution.

The next sections will briefly introduce the reader to the dynamics involved: the motion dynamics (the platform, section II), the perception mechanism (the vestibular system, section III). Then the formalization section will figure out the details of the optimal motion cueing and will defend the authors approach.

Notation

- x or H: medium letters are scalars
- $\mathbf{q}$: bold small letters are vectors
- $\mathbf{M}$: bold capital letters are matrices
- $\widehat{a}$: letters with a hat are perceived variables

2 PLATFORM KINEMATICS AND DYNAMICS

The Gough-Stewart parallel robot is composed of three parts: a moving body (*the platform*) linked to a fixed body (*the base*) through six extensible legs. Each leg is composed of a prismatic joint (i.e. an electro-hydraulic jack) and two passive spherical joints making the connection with the base and the platform (Figure 2 depicts the platform without the cockpit). For an excellent overview of parallel robots the reader is referred to (Merlet, 2000).

Here the task space coordinates $\mathbf{q}$ are used to calculate the dynamical model

$$\mathbf{q} = [x, y, z, \phi, \theta, \psi]^T \tag{1}$$

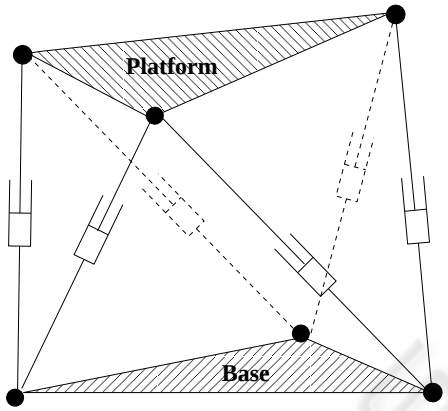

Figure 2: Parallel robot architecture

where (x, y, z) is the platform displacement vector and (ϕ, θ, ψ) are the Euler angles defining its orientation.

The Lagrange-Euler method was adopted to calculate the 6-dimensional nonlinear system figuring the generalized forces vector $\mathbf{f}$

$$\mathbf{M}(\mathbf{q})\ddot{\mathbf{q}} + \mathbf{C}(\mathbf{q}, \dot{\mathbf{q}})\dot{\mathbf{q}} + \mathbf{g}(\mathbf{q}) = \mathbf{f} \tag{2}$$

The symmetric positive semi-definite[2] matrix $\mathbf{M}(\mathbf{q})$ is the mass tensor. $\mathbf{C}(\mathbf{q}, \dot{\mathbf{q}})\dot{\mathbf{q}}$ are the Coriolis and centripetal forces (computed thanks to the Christoffel symbols). $\mathbf{g}(\mathbf{q})$ are the gravity forces (including the platform and the legs weights). Some usual simplification hypotheses were put forward such as: friction neglect, rigid bodies, and identical legs. The dynamical model figuring the actuators forces $\mathbf{u}$ as the input is obtained thanks to the relation (geometrical projection)

$$\mathbf{f} = \mathbf{J}^T(\mathbf{q})\mathbf{u} \tag{3}$$

where $\mathbf{J}(\mathbf{q})$ is the inverse Jacobian matrix[3].

Remark

The level of complexity of the dynamical modeling could be considered as a control parameter. Indeed, some control problems could need high speed processing, conflicting with a slow computational model. The Lagrange-Euler method have an interesting modular approach (based on the kinetic energy separation). This property helps to build easily different degree-of-complexity models.

[2]The use of Euler angles induces purely mathematical singularities at $\theta = \pm\pi/2$.

[3]Singularity issues of the Jacobian matrix are not addressed in this paper (see (Merlet, 2000)).

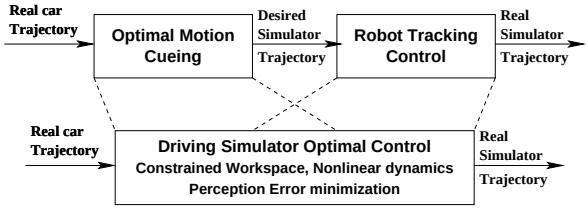

Figure 3: Top diagram: the classical washout strategy. Bottom diagram: the unifying optimal control strategy

3 THE VESTIBULAR SYSTEM

The vestibular system (VS), located in the inner ear, is the inertial motion sensor. This biological apparatus measures both linear and angular motions. The VS is composed of two components: the otoliths and the semicircular canals responsible respectively for longitudinal and for angular cue responses. More precisely, they are sensitive to linear *acceleration* and to angular *speed*. An overview of these organs can be found in (Berthoz and Droulez, 1982; Reymond, 2000). Otoliths have a noteworthy feature: they are sensitive to the acceleration and to the gravity force without the ability of distinction. The well-known "*tilt coordination*", for instance, uses this ambiguity: "*When a visual scene representing an accelerated translation is presented to the driver while the simulation cockpit is tilted at an undetectable rate, the relative variation of the gravity vector will be partly interpreted as an actual linear acceleration*" (Reymond et al, 2000).

Vestibular models

For the longitudinal acceleration restitution (surge) the adopted otoliths model is Telban's (Telban and Cardullo, 2001). It relates the perceived acceleration $\widehat{a}$ (*the hat means perceived*) to the otoliths acceleration:

$$\frac{\widehat{a}}{a_{oto}} = \frac{K(\tau_L s + 1)}{(\tau_1 s + 1)(\tau_2 s + 1)} \tag{4}$$

The involved time constants are $\tau_L = 10s$, $\tau_1 = 5s$ and $\tau_2 = 0.016s$. K is a constant positive gain which can be chosen arbitrarily. The otoliths acceleration can be achieved either by translating the platform in the surge direction x or by tilting it (following the pitch angle θ)

$$a_{oto} = \ddot{x} - g\theta \tag{5}$$

The term '$-g\theta$' is the 'tilt coordination' contribution. Note that the last equation is correct only for constant angular speed and small angular motion.

The semi-circular model (Goldberg and Fernandez, 1971) relates the perceived angular speed $\widehat{\omega}$ to the platform one $\omega = \dot{\theta}$:

$$\frac{\widehat{\omega}}{\omega} = \frac{\tau_a \tau_b s^2}{(\tau_a s + 1)(\tau_b s + 1)} \tag{6}$$

The involved time constants are $\tau_a = 5.7s$ and $\tau_b = 80s$.

4 OPTIMAL CONTROL FORMALIZATION

This section first describes the optimal motion cueing algorithm and then presents the authors extension and contribution. The latter scheme is developed to study offline platform responses, to check maneuvers feasibility and to analyze the evolution and magnitudes of the articular forces. In other words our approach does not address real-time algorithms. Nonetheless it answers the question: given the geometric constraints, what is the best the platform can do?

4.1 Optimal motion cueing

Figure 4 summarizes the optimal washout scheme (referred to as *washout* in the following). Starting from real car trajectories $\mathbf{p}_r$, one have (path 1) the motion perception in a real world configuration. One have as well (path 2) the motion perception caused by the filtered trajectories $\mathbf{p}_s$ (i.e. the trajectories that the platform should track). The goal is to look for a linear washout filter $\mathbf{W}(s)$ that minimizes the perception error i.e. the difference between these two paths.

The trajectories are represented by two parameters: the linear acceleration and the angular speed. Indeed they are the most significant factors for the perception process (as described in section 3). Thus $\mathbf{p}_r = (a_r, \omega_r)$ denotes the real car trajectory and $\mathbf{p}_s = (a_s, \omega_s)$ is the trajectory that should be tracked by the simulator.

The intuitive choice: "$\mathbf{W}(s)$ equals identity" gives a perfect error cancellation. However, due to the platform motion constraints this choice is not feasible. The optimal motion cueing algorithm computes a linear washout filter $\mathbf{W}(s)$ by solving the following minimization problem: Given a filtered Gaussian noise as a real car trajectory, minimize the statistical mean

$$\min_{\mathbf{p}_s} E\left\{ \int_{t_0}^{t_f} \mathbf{e}^T \mathbf{Q} \mathbf{e} + \mathbf{x}_d^T \mathbf{R}_d \mathbf{x}_d + \mathbf{p}_s^T \mathbf{R} \mathbf{p}_s \right\} \tag{7}$$

(The matrices involved in this cost are positive symmetric definite). This cost involves three terms:

- $\mathbf{e}^T \mathbf{Q} \mathbf{e}$: the perception error cost (perception validity)

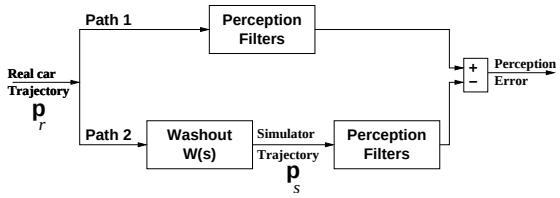

Figure 4: Optimal motion cueing scheme

- $\mathbf{x}_d^T \mathbf{R}_d \mathbf{x}_d$: the platform displacement cost (constrained workspace). It is important to notice that $\mathbf{x}_d$ is ruled by a simple linear system. Indeed, it is tacitly assumed that the platform tracks perfectly the $\mathbf{p}_s$ trajectories. Then $\mathbf{x}_d$ is composed of the integrals of a_s and ω_s.
- $\mathbf{p}_s^T \mathbf{R} \mathbf{p}_s$: another way to account for the constrained workspace.

This algorithm has some drawbacks

- The washout block does not deliver the platform trajectories but the ones that should be tracked. Moreover, the tracking process will induce errors and delays partly caused by the platform dynamical delays and by the actuator coupling. And it appears that it is more relevant and correct to minimize the perception error as a difference between the tracked and the real perceived trajectories. This is done in the unifying optimal control approach by including a nonlinear dynamical model in the optimization algorithm
- The actuator controls are constrained. However these constraints are not directly included in the washout algorithm. This may cause problems, for instance: what if the desired trajectories are geometrically feasible but the constraints on the controls are not respected ?
- The washout algorithm does not use the 'tilt coordination'. Indeed, for instance, if the real car performs a linear acceleration, the trajectory delivered by the washout will also be a linear simulator acceleration (without any variation of the tilt angle)
- Motion cueing algorithms were primarily designed for flight simulators. However "the dynamics of land vehicle are very different the one of an aircraft. Land vehicles are usually much faster if compared to the one of a large aircraft. This is due to a higher power to mass ratio and to the specific nature of moving on the ground, where higher friction is present" (Barbagli, 2001). This quick dynamics (instantaneous breaks and accelerations) shows the limitation of using a linear washout and motivates exploring non-linear transformations.

4.2 Unifying optimal control approach

In order to account for the last points, this paper unifies the two blocks: control and washout filtering. Thanks to the knowledge of the dynamical model (2), (3) and the vestibular filters (4), (6), the authors propose to find the optimal actuator controls needed to minimize

$$\min_{\mathbf{u}} \left\{ \int_{t_0}^{t_f} \mathbf{e}^T \mathbf{Q} \mathbf{e} + \mathbf{x}_d^T \mathbf{R}_d \mathbf{x}_d + \mathbf{u}^T \mathbf{R} \mathbf{u} \right\} \quad (8)$$

Compared with the former cost (7)

- This is a deterministic approach. The goal is not to find a washout filter, but to compute directly the optimal actuator forces
- The perception error $\mathbf{e}$ is now the difference between the real simulator and the real car trajectories
- The displacement vector $\mathbf{x}_d$ is ruled by the nonlinear model (2): $\mathbf{x}_d = (\mathbf{q}, \dot{\mathbf{q}})$
- The cost $\mathbf{p}_s^T \mathbf{R} \mathbf{p}_s$ is replaced by a cost on the actuator forces $\mathbf{u}^T \mathbf{R} \mathbf{u}$ (so that one can act directly on them)

Remarks

- Other choices of $\mathbf{x}_d$ are possible. Indeed one can select from $(\mathbf{q}, \dot{\mathbf{q}})$ the relevant components with respect to the experiment. For instance, in the case of a pitch motion restitution, a possible choice of $\mathbf{x}_d$ is $(\theta, \dot{\theta})$, since the remaining degrees of freedom should not be used.
- Besides the choice of the weights, this control is parameterized by the dynamical model, the choice of the vestibular filters, the choice of $\mathbf{x}_d$.

5 OPTIMAL CONTROL CALCULATION AND RESOLUTION

This section details the calculation and the resolution of the optimal control problem. The whole system (figuring the platform dynamics and the perception mechanism) can be described by a first order system with a linear dependence on $\mathbf{u}$. Then, a simple theoretical expression for the optimal control $\mathbf{u}^*$ is obtained. Eventually, the resolution scheme is formulated as a boundary value problem.

5.1 Preliminaries

First of all, let us separate the control $\mathbf{u}$ into the *effective* control $\mathbf{u}_e$ and the weight compensation control $\mathbf{u}_g$:

$$\mathbf{u} = \mathbf{u}_e + \mathbf{u}_g,\ \mathbf{u}_g = \mathbf{J}^{-T}(\mathbf{q})\mathbf{g}(\mathbf{q}) \quad (9)$$

Then, from (2) and (3) the new dynamical equations involving $\mathbf{u}_e$ are

$$\mathbf{J}^{-T}(\mathbf{q})\mathbf{M}(\mathbf{q})\ddot{\mathbf{q}} + \mathbf{J}^{-T}(\mathbf{q})\mathbf{C}(\mathbf{q},\dot{\mathbf{q}})\dot{\mathbf{q}} = \mathbf{u}_e \quad (10)$$

This model is used to compute the optimal control. Secondly, this second order system is converted to a first order system with a new state variable

$$(\mathbf{x}_1, \mathbf{x}_2) = (\mathbf{q}, \dot{\mathbf{q}}) \quad (11)$$

$$\begin{pmatrix} \dot{\mathbf{x}}_1 \\ \dot{\mathbf{x}}_2 \end{pmatrix} = \begin{pmatrix} \mathbf{x}_2 \\ \mathbf{a}(\mathbf{x}_1,\mathbf{x}_2) \end{pmatrix} + \begin{pmatrix} \mathbf{0}_{6\times 6} \\ \mathbf{B}(\mathbf{x}_1) \end{pmatrix} \mathbf{u}_e \quad (12)$$

$\mathbf{a}$ and $\mathbf{B}$ are respectively a 6-dimensional vector and matrix

$$\mathbf{a}(\mathbf{x}_1,\mathbf{x}_2) = -\mathbf{M}^{-1}(\mathbf{x}_1)\mathbf{C}(\mathbf{x}_1,\mathbf{x}_2)\mathbf{x}_2 \quad (13)$$

$$\mathbf{B}(\mathbf{x}_1) = \mathbf{M}^{-1}(\mathbf{x}_1)\mathbf{J}^T(\mathbf{x}_1) \quad (14)$$

Thanks to this linear dependence on $\mathbf{u}_e$, a simple theoretical expression for the optimal control is obtained. Secondly, the robot is assumed to start from the initial configuration $\mathbf{q}_0$[4]. This initial point is a good estimate of the 6-dimensional workspace center. Thirdly, a 4-dimensional state-space representation is derived from the vestibular filters (4) and (6) presented in section 3:

$$\begin{cases} \dot{\mathbf{x}}_3 = \mathbf{A}_{ves}\mathbf{x}_3 + \mathbf{B}_{ves}\,(\dot{\theta},\dot{x})^T \\ (\widehat{a},\widehat{\omega})^T = \mathbf{C}_{ves}\mathbf{x}_3 + \mathbf{D}_{ves}\,(\dot{\theta},\dot{x})^T \end{cases} \quad (15)$$

And finally the target is the final time t_f. Let us define the overall optimal control state variable

$$\mathbf{x} = (\mathbf{x}_1^T, \mathbf{x}_2^T, \mathbf{x}_3^T)^T \quad (16)$$

The system then have a first order structure

$$\dot{\mathbf{x}} = \mathbf{f}(\mathbf{x}) + \mathbf{G}(\mathbf{x})\mathbf{u}_e \quad (17)$$

Note that the drift dynamics $\mathbf{f}(\mathbf{x})$ (used in the last equation) should not be confused with the generalized forces $\mathbf{f}$ (in equation (2)).

5.2 Formalization

The overall cost to be minimized is as follows

$$J(\mathbf{x}_0,\mathbf{u}_e) = \int_{t_0}^{t_f} J_t(\mathbf{x}(t),\mathbf{u}_e(t),t)dt \quad (18)$$

where the continuous criterion J_t is the sum of squared quadratic norms on the control magnitude, the distance from the neutral configuration $\mathbf{q}_0$ and the perception error. Let's define

$$\mathbf{x}_d = \mathbf{q} - \mathbf{q}_0,\ \mathbf{e} = (\hat{a} - \hat{a}_r, \hat{\omega} - \hat{\omega}_r)^T \quad (19)$$

$(\hat{a},\hat{\omega})$ are the perceived acceleration and angular speed provided by the platform whereas $(\hat{a}_r,\hat{\omega}_r)$ are the reference perceived trajectories i.e. the perception of a real car trajectory. Then the cost is

$$J_t = \mathbf{e}^T\mathbf{Q}\mathbf{e} + \mathbf{x}_d^T\mathbf{R}_d\mathbf{x}_d + \mathbf{u}_e^T\mathbf{R}\mathbf{u}_e \quad (20)$$

Writing the Hamiltonian

$$H = J_t(\mathbf{x},\mathbf{u}_e) + \lambda^T\mathbf{f}(\mathbf{x}) + \lambda^T\mathbf{G}(\mathbf{x})\mathbf{u}_e \quad (21)$$

(λ is the 16-dimensional vector of the Lagrange multipliers) shows its quadratic dependence on $\mathbf{u}_e$, thus allowing a straightforward formula for the optimal control $\mathbf{u}_e^*$

$$\mathbf{u}_e^* = -\frac{1}{2}\mathbf{R}^{-1}\mathbf{G}^T\lambda \quad (22)$$

Eventually, the whole boundary value problem is built. It consists of a 32-equation system:

$$\dot{\mathbf{x}} = \mathbf{f}(\mathbf{x}) + \mathbf{G}(\mathbf{x})\mathbf{u}_e^*,\ \dot{\lambda} = -\frac{\partial H}{\partial \mathbf{x}}(\mathbf{x},\lambda,\mathbf{u}_e^*,t) \quad (23)$$

and the boundary conditions composed of the initial and the transversality conditions

$$\mathbf{x}(t_0) = \mathbf{x}_0,\ \lambda(t_f) = 0 \quad (24)$$

6 SIMULATIONS

The Matlab© function 'bvp4c' was used to solve this boundary value problem. A passing maneuver was simulated. A nonlinear platform dynamical model with null-weighted legs was implemented.

Scenario

In the virtual world, the driver was provided prior motion and visual cues to give him the feeling of driving at a constant speed. Now the robot is motionless at its neutral position and the visual scene provides entirely the motion illusion. Starting from this situation, the driver accelerates to overtake a car and then decelerates to restore his cruise speed. Two experiments were carried out to simulate this manoeuvre: with and without the use of the tilt coordination. Both tests used the same weight matrices involved in the cost (8). These weights were chosen so that, the platform can go near to its displacement limits[5]. Consequently, they enable a good exploitation of the simulator capabilities.

[4] The neutral position $\mathbf{q}_0$ can also be considered as a control parameter.

[5] See the introduction section for the values.

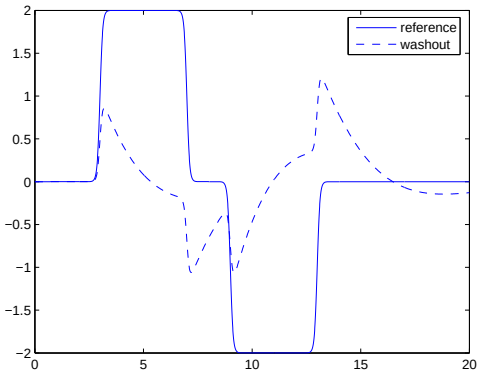

Figure 5: Real reference acceleration and washout acceleration (ms^{-2})

Real values

This virtual scenario have a corresponding car trajectory in the real world. Figure 5 depicts

- the real car acceleration trajectory a_r (solid line). The otoliths filter response to this trajectory is the reference perception trajectory.
- the desired simulator trajectory a_s delivered by the washout (dashed line). This plot shows that the washout is a high-pass filter that could induce significant false cues (such as its responses at $t = 7s$ and $t = 13s$).

6.1 Without 'tilt coordination'

In this experiment, only the linear platform motion is used to render the linear acceleration.

Comparing the motion perceptions

Figure 6 plots three perceived accelerations: the reference $\widehat{a}_r$, the optimal scheme $\widehat{a}$ (simulator, solid line) and the washout $\widehat{a}_s$.
The authors scheme has three features:

- A backward platform motion (in $\widehat{a}$) precedes the desired forward one (see the first 3 seconds in Fig.6). The platform goes back to perform better forward acceleration. This could be explained by the cost on the displacement $\mathbf{x}_d^T \mathbf{R}_d \mathbf{x}_d$ ($\mathbf{x}_d = \mathbf{q} - \mathbf{q}_0$). Indeed it acts like a spring pulling the simulator to its neutral position $\mathbf{q}_0$. The same comment holds for the acceleration behavior at $t = 9s$.
- The optimal control scheme acts like a high-pass filter. The sustained parts in the reference acceleration $\widehat{a}_r$ are completely canceled. This is natural since the displacement is highly constrained.
- Thirdly, the optimal control amplitude is lesser than the washout (dynamical limitation).

Other analysis

Figure 7 depicts the effective actuator forces $\mathbf{u}_e^*$ (without the weight compensation forces). It presents fast variations up to 350N. Figure 8 shows that the simulator displacement, speed and acceleration are within the constrained workspace.

Conclusion The constrained workspace altered considerably the rendering of the acceleration perception.

6.2 With 'tilt coordination'

In this simulation, both linear motion and tilt coordination were used to render the linear acceleration.

Comparing the motion perceptions

Figure 9 shows an excellent rendering of the acceleration perception. The 'tilt coordination' is indeed essential in this experiment. The tilt contributes considerably to the perception (Fig.12) despite a very reduced angular motion (Fig.13). It enables the restitution of the low-frequency part that could not be performed by the linear motion.

Other analysis

As the 'tilt coordination' shares the restitution task with the linear motion, the latter have lesser amplitudes (see Fig.11) than the former test (without tilt). The actuator controls are lesser as well (see Fig.10).

Conclusion The 'tilt coordination' is a powerful trick to circumvent the workspace constraints. Very good results are achieved.

7 CONCLUSION

The purpose of the this paper is to develop an optimal control approach that extends and over-perform the optimal motion cueing algorithm. A nonlinear dynamical model was built. Vestibular filters and the 'tilt coordination' trick were included in the algorithm. Simulations showed the influence of the nonlinear dynamics and the importance of 'tilt coordination'. Future works will deal with the vestibular-visual interaction. Robustness shall also be studied by integrating modelling errors and computation delays.

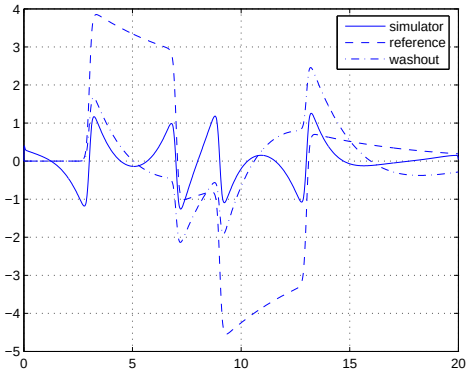

Figure 6: No tilt: perceived accelerations

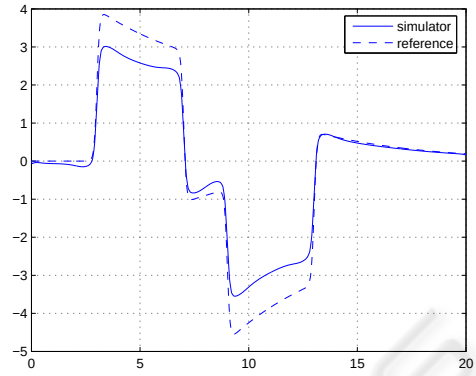

Figure 9: With tilt: perceived accelerations

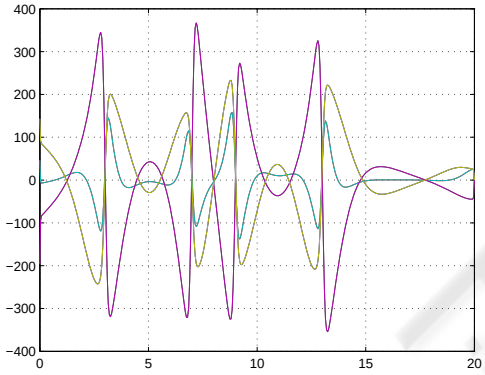

Figure 7: No tilt: $\mathbf{u}_e^*$ actuator forces N

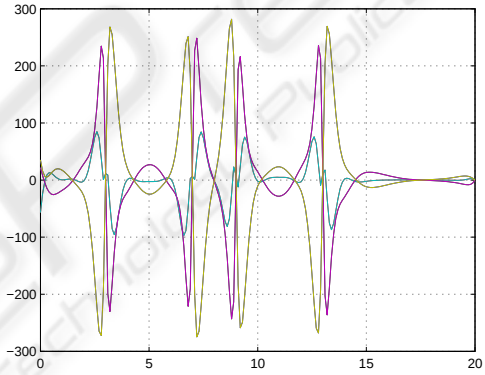

Figure 10: With tilt: $\mathbf{u}_e^*$ actuator forces N

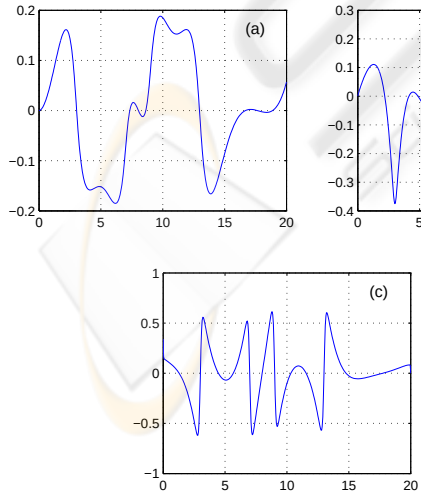

Figure 8: No tilt: (a) platform displacement m, (b) platform speed ms^{-1}, (c) platform acceleration ms^{-2}

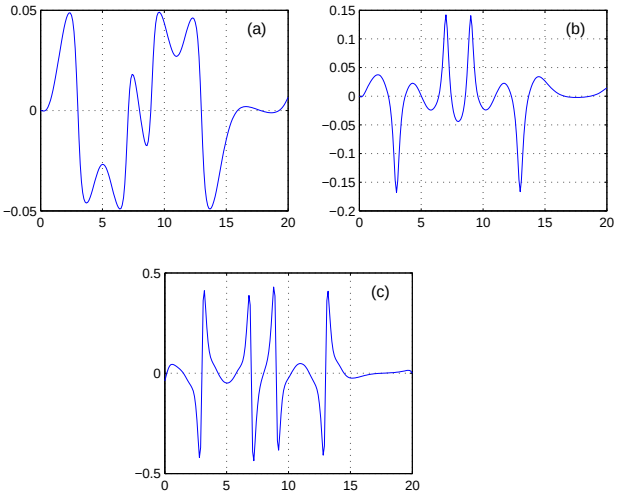

Figure 11: With tilt: (a) platform displacement m, (b) platform speed ms^{-1}, (c) platform acceleration ms^{-2}

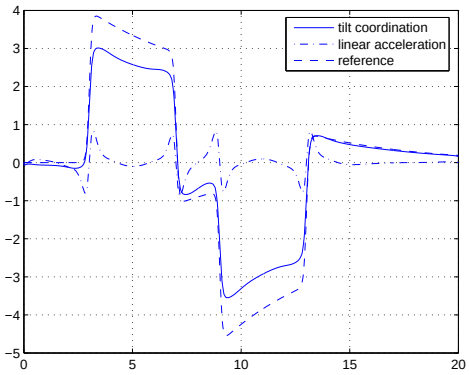

Figure 12: With tilt: linear acceleration and tilt coordination contributions to the perception restitution

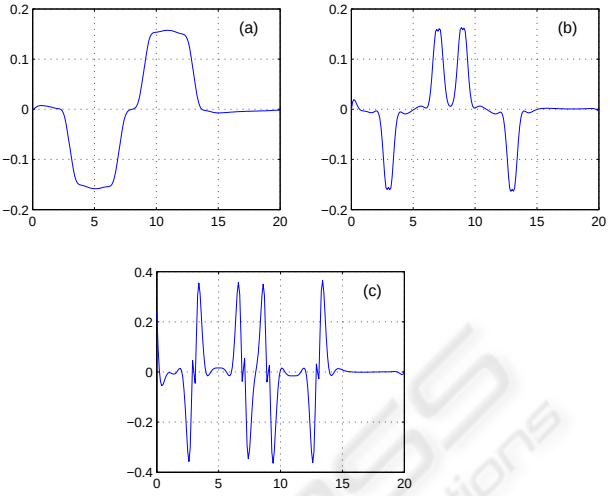

Figure 13: With tilt: (a) tilt angle rd, (b) tilt speed rds^{-1}, (c) tilt acceleration rds^{-2}

ACKNOWLEDGMENT

This work has been supported by the French ministry of transportation in the framework of the PREDIT programme 2002-2006: HybriSim project.

REFERENCES

Barbagli, F. et al (2001). Washout filter design for a motorcycle simulator. In *IEEE Computer Society, Proceedings of the Virtual Reality 2001 Conference*, pages 225–232, Yokohama, Tokyo.

Berthoz, A. and Droulez, J. (1982). Linear self-motion perception. *Tutorials on Motion Perception*, A.H. Wertheim, W.A. Wagenaar and H.W. Leibowitz (eds.), Plenum, New York.

Cardullo, F.M. et al (1999). Motion cueing algorithms: A human centered approach. *5th International Symposium on Aeronautical Sciences*, Zhukovsky, Russia.

Goldberg, J. and Fernandez, C. (1971). Physiology of peripheral neurons innervating semicircular canals of the squirrel monkey. ii. response to sinusoidal stimulation and dynamics of peripheral vestibular system. *Journal of Neurophysiology*, 34:661–675.

Guo, L. et al (2003). The results of a simulator study to determine the effects on pilot performance of two different motion cueing algorithms and various delays, compensated and uncompensated. *American Institute of Aeronautics and Astronautics: Modeling and Simulation Technologies Conference and Exhibit*, Austin, Texas.

Merlet, J.-P. (2000). *Parallel Robots*, volume 74 of *Solid mechanics and its applications*. G.M.L. Gladwell (ed), Kluwer Academic Publishers.

Reymond, G. et al (2000). Validation of Renault dynamic simulator for adaptive cruise control experiments. *Proceedings of the Driving Simulation Conference*, pages 181–191, Paris.

Reymond, G. (2000). *Contribution des stimulis visuels, vestibulaires et proprioceptifs dans la perception du mouvement du conducteur*. PhD thesis, Neurosciences department, Université Paris VI - Renault.

Telban, R.J. et al (1999). Developments in human centered cueing algorithms for control of flight simulator motion systems. *American Institute of Aeronautics and Astronautics: Modeling and Simulation Technologies Conference and Exhibit*, Portland. OR.

Telban, R.J. and Cardullo, F.M. (2001). An integrated model of human motion perception with visual-vestibular interaction. *American Institute of Aeronautics and Astronautics: Modeling and Simulation Technologies Conference and Exhibit*, Montreal, Canada.

Telban, R.J. and Cardullo, F.M. (2002). A nonlinear, human-centered approach to motion cueing with a neurocomputing solver. *American Institute of Aeronautics and Astronautics: Modeling and Simulation Technologies Conference and Exhibit*, Monterey, California.